Assessment of consistent two-equation closure for forest flows

Sogachev, Andrey; Cavar, Dalibor; Bechmann, Andreas; Ejsing Jørgensen, Hans

Publication date:
2015

Document Version
Publisher's PDF, also known as Version of record

ASSESSMENT OF CONSISTENT TWO-EQUATION CLOSURE FOR FOREST FLOWS

Andrey Sogachev

Wind Energy Department, Technical University of Denmark, Building 118, P.O. Box 49, Frederiksborgvej 399, DK-4000, Roskilde, Denmark.
anso@dtu.dk, tel: +45 2133 1197, fax: +45 4677 5083.

Co-author(s): Dalibor Cavar (1), Andreas Bechmann (1), Hans Ejsing Jørgensen (1)

(1) Wind Energy Department, Technical University of Denmark, Roskilde, Denmark

Summary

The paper reports on modelling of air flow over the forested area of Østerild in Denmark using two different CFD models with a consistent two-equation closure. Being consistent with the canonical flow regimes of grid turbulence and wall-bounded flow, the closure used is also valid for homogeneous shear flows commonly observed inside tall vegetative canopies. The numerical experiments show that the treatment of plant drag in the closure has universality and can be applied on any two-equation closure. Results derived by different CFD models with k-epsilon and k-omega closure are similar and in good comparison with observations. Overall, numerical results show that the closure performs well, opening new possibilities for application to tasks related to the atmospheric boundary layer - where it is important to adequately account for the influence of vegetation.

Introduction

The two-equation closure approach, based on coupled transport equations for the turbulent kinetic energy (TKE), k, and a supplementary length-scale determining variable φ (typically the dissipation rate), provides the minimum level of complexity capable of simulating the effective turbulence length scale, ℓ, as a dynamic variable - the condition needed to adequately simulate airflow over complex terrain [1]. Having a relatively low computational cost, this approach appears to be the optimal choice for practical tasks where “the interaction and joint effects of heterogeneities are more interesting than a highly detailed description of the turbulence field” [2] and/or where uncertainty introduced by underlying surface (e.g. forest properties) “limit the accuracy of modelled wind statistics, regardless of the turbulence closure chosen” [3].

In spite of the appealing properties mentioned above, the two-equation closure methodology received limited attention in atmospheric research, as opposed to its widespread use in computational fluid dynamics (CFD) research and industrial applications [4, 5]. Applications of CFD methodology to atmospheric flows have highlighted the need to adapt governing equations and turbulence closures for atmospheric boundary layer (ABL) flows [6]. For example, in dealing with the heterogeneity of real landscape, one is mainly faced with the problem of modelling inhomogeneous flow over vegetation, but the fundamental uncertainty about how to treat the vegetative-drag effect in a most suitable manner, is still the main problem in development of a model(s) capable to simulate such flows [2, 7].

In recent years, more and more wind farms were located on forested sites where the forest has a significant impact on power production and creates challenges in assessing the wind resource. Forested sites significantly reduce wind velocity and increase turbulence. Addressing this, DTU Wind Energy have developed the CFD parameterization for drag effects of vegetation for many years. The atmospheric boundary layer (ABL) model SCADIS [8, 9] is a basic tool for such kind of investigation. Due to its flexibility, SCADIS allows testing of any assumption in an easy and straightforward way. However, the model is designed for a single processor and cannot be used on a massive computing scale, needed for wind industry. DTU Wind Energy’s

other in-house CFD solver - EllipSys3D [10, 11] have however been designed for massive parallel computing. Based on our SCADIS experience, EllipSys3D was improved in order to simulate forested ABL flow problems.

The objectives of present study are i) to implement the consistent two-equation closure treating plant drag effects in EllipSys3D and ii) to test and validate the performance of updated EllipSys3D ($k-\varepsilon$ closure) against SCADIS ($k-\omega$ closure) and observations from the Østerild National Test Centre, located on a coastal plain in Denmark.

Mathematical models

Although each CFD model considered in this study has its own specific properties regarding the levels of physics described and the basic computational approach, the governing equations used are similar, except for some minor details (e.g. in SCADIS air density is constant). Here we will concentrate on the closure issues and implementation of vegetation effect, thus only equations, modified due to plant drag effect, are presented. These are [9]:
The momentum equation,

$$\frac{\partial\langle \overline{u}_i\rangle}{\partial t}+\langle\overline{u}_j\rangle\frac{\partial\langle\overline{u}_i\rangle}{\partial x_j}+2\varepsilon_{ijk}\Omega_j\langle\overline{u}_k\rangle+\frac{\partial\langle\overline{P}\rangle}{\partial x_i}+\frac{\partial\langle\overline{u_i'u_j'}\rangle}{\partial x_j}=S_i; \tag{1}$$

The transport equation for turbulent kinetic energy (TKE), k,

$$\frac{\partial k}{\partial t}+\langle\overline{u}_j\rangle\frac{\partial k}{\partial x_j}-\frac{\partial}{\partial x_i}\left(\frac{\mu_t}{\sigma_E^{\varphi}}\frac{\partial k}{\partial x_i}\right)-\left(P_k-\varepsilon\right)=S_p-S_d=0\ ; \tag{2}$$

The transport equation for supplemented variable φ, needed for derivation of eddy viscosity, μ_t.

In EllipSys3D such variable is usually the rate of dissipation of TKE, ε, i.e.

$$\begin{aligned}\frac{\partial\varepsilon}{\partial t}+\langle\overline{u}_j\rangle\frac{\partial\varepsilon}{\partial x_j}-\frac{\partial}{\partial x_i}\left(\frac{\mu_t}{\sigma_\varepsilon}\frac{\partial\varepsilon}{\partial x_i}\right)-\frac{\varepsilon}{k}\left(C_{\varepsilon1}P_k-C_{\varepsilon2}\varepsilon\right)\\ =\frac{\varepsilon}{k}(C_{\varepsilon1}-C_{\varepsilon2})\left(-\ell/\ell_e\right)P_k-\frac{\varepsilon}{k}\left(C_{\varepsilon1}-C_{\varepsilon2}\right)S_d+D,\end{aligned} \tag{3}$$

and in SCADIS the specific dissipation of TKE, $\varphi=\omega=\varepsilon/k$, is used, i.e.

$$\begin{aligned}\frac{\partial\omega}{\partial t}+\langle\overline{u}_j\rangle\frac{\partial\omega}{\partial x_j}-\frac{\partial}{\partial x_i}\left(\frac{\mu_t}{\sigma_\omega}\frac{\partial\omega}{\partial x_i}\right)-\frac{\omega}{k}\left(C_{\omega1}P_k-C_{\omega2}\omega k\right)\\ =\frac{\omega}{k}(C_{\omega1}-C_{\omega2})\left(-\ell/\ell_e\right)P_k-\frac{\omega}{k}\left(C_{\omega1}-C_{\omega2}\right)S_d.\end{aligned} \tag{4}$$

In Eqs. (1 - 4) x_i ($x_1 = x$, $x_2 = y$, $x_3 = z$) are the longitudinal, lateral and vertical directions, respectively; u_i ($u_1 = u$, $u_2 = v$, $u_3 = w$) are the velocity components along x_i; P is the kinematic pressure; $\varepsilon_{ijk}\Omega_j$ is the Earth's rotation tensor. An overbar and angle brackets denote time and horizontal averaging, respectively; a prime is used for the deviation from the time average. σ_E^{φ} and σ_φ are the Schmidt numbers for k and φ ($\varphi \equiv \varepsilon, \omega$), respectively (with σ_E^{φ} also depending on the φ equation used for closure). P_k is the rate of shear production, and $C_{\varphi1}$ and $C_{\varphi2}$ are conventional coefficients of production and destruction terms in the equation for φ, [12].

The mixing length, ℓ, and the eddy viscosity, μ_t, are expressed in terms of k and ε as

$$\ell = \frac{C_\mu^{3/4} k^{3/2}}{\varepsilon}, \tag{5}$$

$$\mu_t = C_\mu \frac{k^2}{\varepsilon} \tag{6}$$

where ε can be obtained from φ, and the closure constant C_μ equals the squared ratio of equilibrium shear stress to TKE. With C_μ = 0.09, other model constants are (σ_k^ε, σ_ε, $C_{\varepsilon 1}$, $C_{\varepsilon 2}$) = (1, 1.7, 1.52, 1.833) and (σ_k^ω, σ_ω, $C_{\omega 1}$, $C_{\omega 2}$) = (1.7, 1.7, 0.52, 0.833) [9].

Considering only terms on the left side of Eqs. (1 - 4), we have standard set of equations used in CFD, that provide log-law velocity profile in the surface layer. The right part consider additional terms that are responsible for ABL and vegetation effects. There are

i) In Eq. (1) the momentum sink of canopy elements, S_i, is usually parameterized as in [13]

$$S_i = -c_d A\langle \overline{u}_i \rangle U, \tag{7}$$

where $U = \left(\langle \overline{u}_i \rangle \langle \overline{u}_i \rangle\right)^{1/2}$ is the absolute value of the spatial and temporal average of the wind speed, c_d is the drag coefficient including the shelter effect and $A(z)$ is the projected leaf area per unit volume (leaf area density – LAD).

ii) In Eq. (2) S_p and S_d are wake production and enhanced dissipation due to the surface drag of canopy elements, respectively [13, 14]. Based on the findings of [2, 15] that S_p = S_d the equation for TKE holds it standard form for canopy flow.

iii) First terms on the right side of Eqs. (3 - 4) modify the closure for ABL conditions limiting the rate of shear production, P_k, when mixing length (i.e. turbulent eddy size) reaches its limiting or equilibrium value, ℓ_e [6]. With $\ell_e = 0.00027 G / f$ (where G is the geostrophic wind speed and f is the Coriolis parameter [16]), this modification allows a natural transition from the standard two-equation model, while satisfying the log-law velocity profile in the surface layer and providing a suitable model solution for the whole neutrally stratified ABL over a plain surface.

iv) Second terms on the right side of Eqs. (3 - 4) implement only the effect of the enhanced dissipation, S_d, on ε or ω. According to [2] the effect of wake production S_p on the total shear production and dissipation of TKE, at least for neutrally stratified conditions, can be ignored. Suggested expression for S_d is [2]

$$S_d = 12 C_\mu^{0.5} c_d A(z) |U| k. \tag{8}$$

v) The third term on the right side of Eq. (3) is extra-diffusion term that provide consistency between $k - \varepsilon$ and $k - \omega$ models. In this study, we adopt the SCADIS solver using k - ω closure, which is thoroughly validated for neutral canopy flows, as a reference model. This is a reason why no third term on the right-hand side of Eq. (4) can be seen. The expression for D is [9, 17]

$$D = C_\mu \left[\left(\frac{1}{\sigma_k^\varepsilon} - \frac{1}{\sigma_\omega} \right) k \frac{\partial^2 k}{\partial x_i^2} - \left(\frac{1}{\sigma_k^\varepsilon} + \frac{1}{\sigma_\omega} \right) \frac{k}{\varepsilon} \frac{\partial \varepsilon}{\partial x_i} \frac{\partial k}{\partial x_i} + \frac{2}{\sigma_k^\varepsilon} \frac{\partial k}{\partial x_i} \frac{\partial k}{\partial x_i} \right]. \tag{9}$$

With the exception of conventional parameterization for momentum sink of canopy elements (i) all other modifications considered above are still debated. All new terms introduced on the right-hand side of the equation can be easily implemented in standard (commercial) CFD code, as extra source/sink terms.

In SCADIS the computational algorithm is designed for transient flow problems, while EllipSys3D in the neutral flow cases can provide both steady-state and transient flow solution.

Case study

The Østerild National Test Centre for Large Wind Turbines is located on a coastal plain, in northern Jutland, Denmark (Fig. 1a). The terrain is flat, except for a small hill in the southwest direction and some sand dunes to the north. The elevations of the test area range from approximately 12 to 14 m ASL. The site has grasslands, and forests in the southern half of the test site with canopy heights between 10 m and 20 m (Fig. 1b). The surroundings are dominated by the North Sea, which is approximately 4 km to the north and 20 km to the west. There is also the Limfjord entrance about 6 km to the southeast.

The Østerild test centre had three wind Lidars installed on the site with wind data recorded between 28/01/2010 and 05/11/2011. In addition to Lidar measurements, two 45-meter-high measuring masts were installed at the West (Fig. 1b) and South measurement positions. These masts were instrumented with sonic and cup anemometers, thus the wind speed profiles for the first 40m are available for later analysis, as the Lidar cannot measure below this altitude. Besides instruments for wind speed and direction, the masts were instrumented with sensors for measuring temperature, rain, humidity and radiation [18, 19].

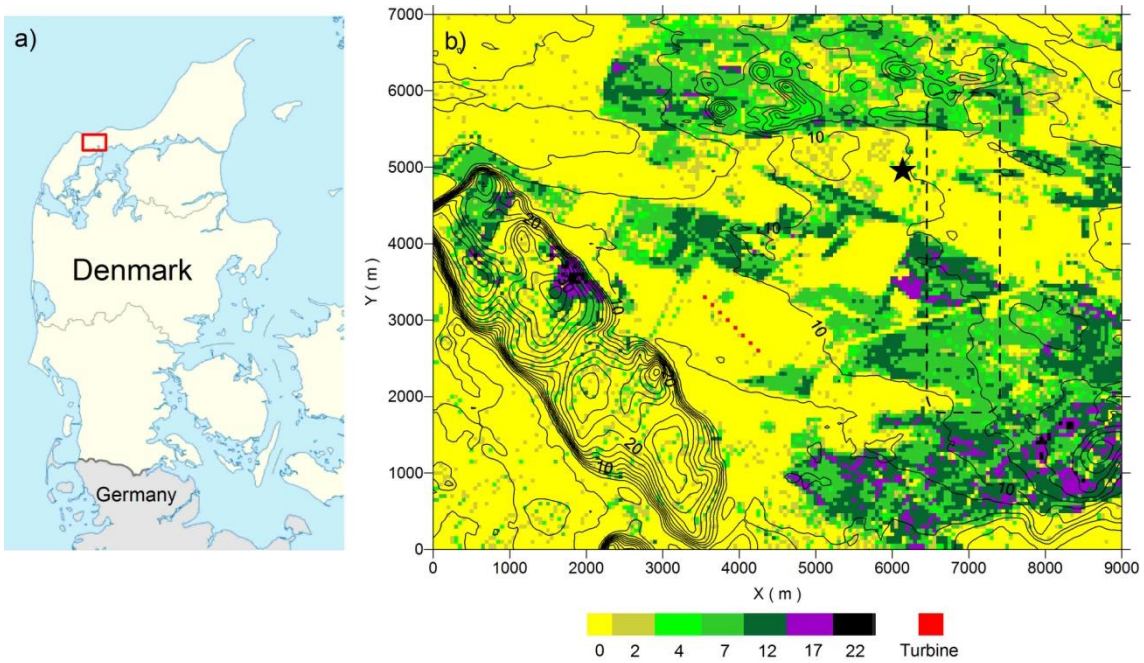

Fig.1. Location of Østerild area (a) and overview of topography (lines) and landuse classes used in the model domain (b). Landuse classes are presented by vegetation of different heights (colour scale) having also different canopy shape and leaf area index. Dashed line indicate area of the Østerild National Test Centre. A row of eight wind turbines west of test stand is also presented. The star is for the West mast.

Numerical results

The SCADIS solution is based on a finite difference numerical approach, while EllipSys3D utilizes a finite volume numerical scheme. To make results comparable, we used an upwind discretization scheme for the advection term in EllipSys3D, as this is the only option in SCADIS. For the same reason, all other numerical parameters used in EllipSys3D were kept identical to the ones used in SCADIS, including the equidistant horizontal resolution of 50 m. An initial condition for wind speed was also identical and specified for flat plain terrain with aerodynamic roughness of 0.03 m, with western geostrophic wind of G = 10 m s^{-1}, at the upper border of the modelling domain (5 km).

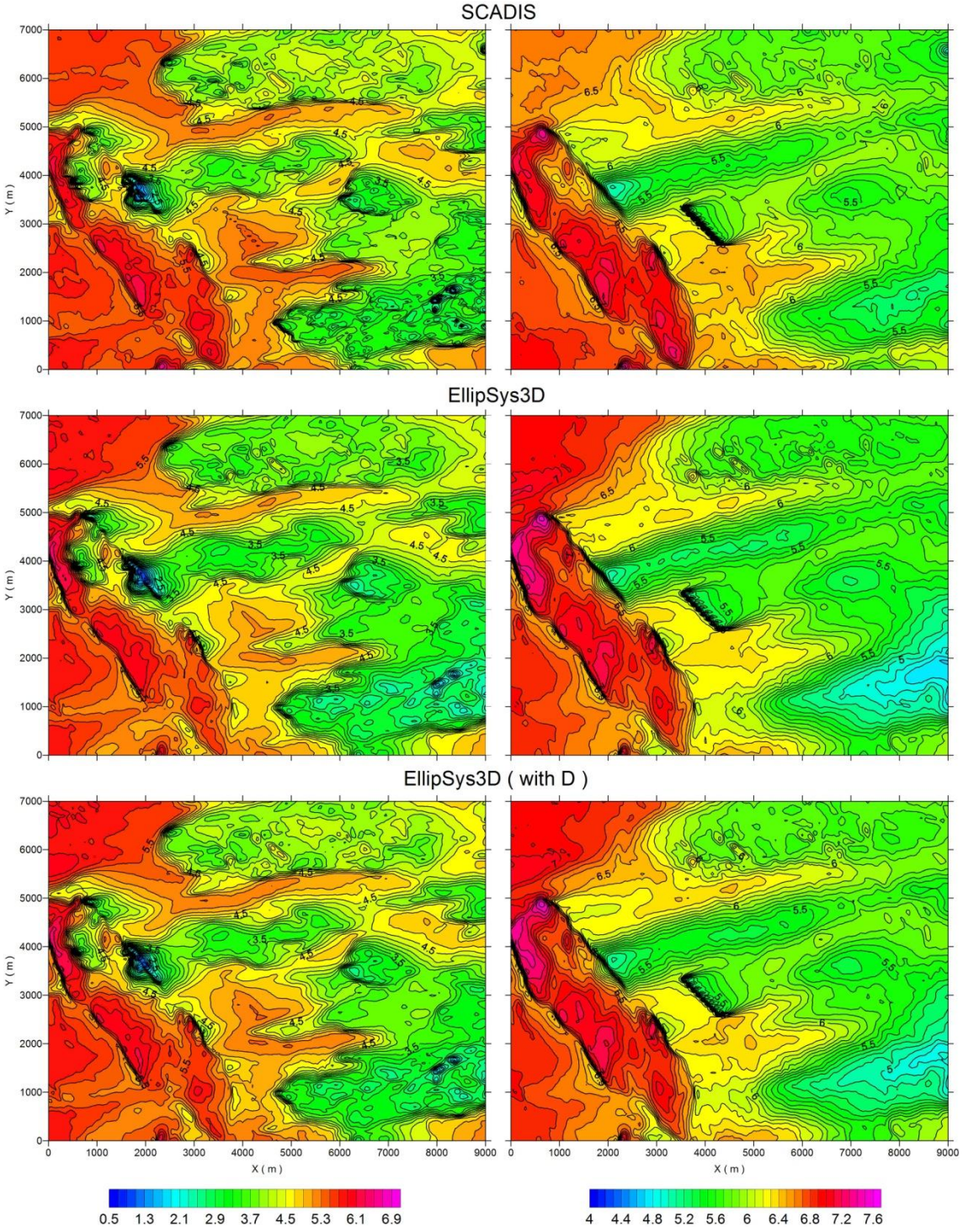

Fig.2. Simulated wind speed (m s^{-1}) at 20 m AGL (on the left side) and at 50 m AGL (on the right side) over Østerild area using different models.

The results of the numerical experiments presented in Fig. 2 show that the two models produced similar wind speeds over investigated domain. Effects of vegetation on the flow are clearly seen. The interpolation algorithm used in EllipSys3D for conversion of vertex-provided information about forest elements to volume cell centres can explain some smoothing effects in

presented results. However, the effect is minor and the scatter plot in Fig. 3a confirms that the two model results are close. Careful inspection of Fig. 2 (especially for 50 m AGL) shows that there are differences in the wind speeds in the area surrounding the hill located upwind of the wind turbines. This is where the terrain following coordinate system implemented in SCADIS is not fully correct.

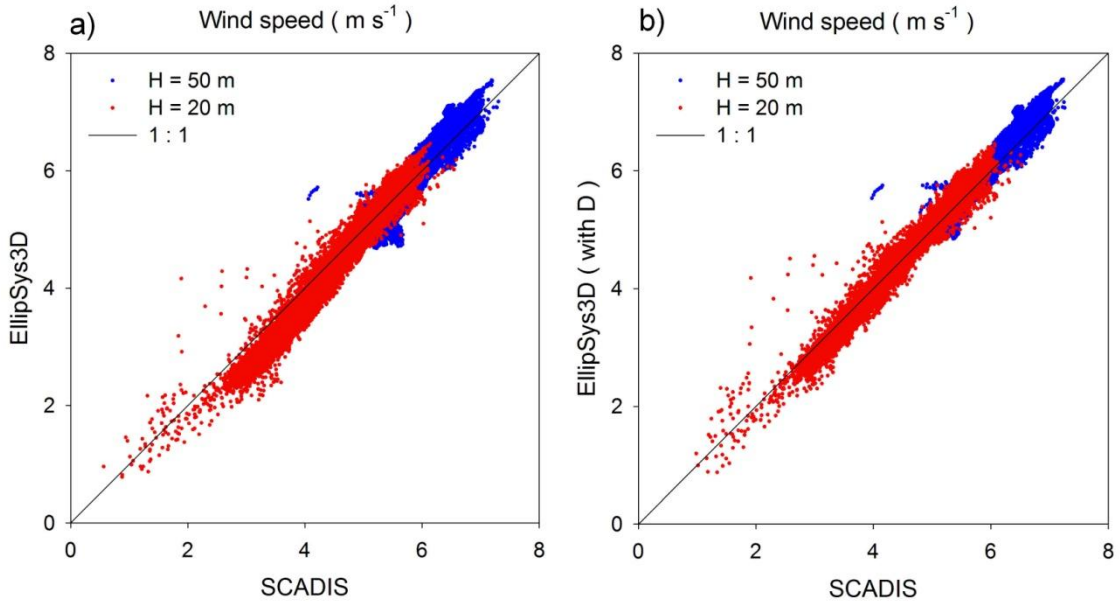

Fig.3. Wind speed at 20 m AGL (red) and at 50 m AGL (blue) derived using the SCADIS model against that derived using the EllipSys3D model over computational domain. The 1 : 1 line is also shown.

The results of numerical experiments presented in Fig. 4 show that both models are similar in description of effect of vegetation on turbulence, even though some differences in absolute values of calculated TKE can be seen. One can observe indeed, that the forest increases turbulence intensity. The areas of high values of TKE are located just above the forest (Fig. 4 LHS) and spread downwind with the increasing heights (Fig. 4 RHS). The areas with denser and higher forest indicate the larger effect on the TKE production. Smoothing effect in the TKE field observed in EllipSys3D results have the same reason, as previously discussed in the case of wind speed field. The difference between $k - \varepsilon$ and $k - \omega$ closures are larger if the TKE gradients are larger. This is why the areas of largest differences in the TKE values between two models correspond to the areas with highest and most dense forest (see also Fig. 1). Fig.5a demonstrates that the largest difference in TKE values between the two models is when TKE have a large value (usually just above treetops). Overall effect is that TKE modelled by EllipSys3D is lower than TKE modelled by SCADIS, even though modelled wind speeds are similar.

Authors of [9] described this effect and provided its possible improvements by implementation of an extra-diffusion term in the equation for dissipation rate of $k - \varepsilon$ closure. Implementing the extra diffusion term in $k - \varepsilon$ model, D, as suggested in [9] (see Eqs. (3) and (9)) provides better agreement between the results of different models (Figs. 3b and 5b), especially for TKE values (see Fig. 4 (lower panels) and Fig. 5b). As the EllipSys3D is more often (traditionally) used in $k - \varepsilon$ standard formulation, it was worth to investigate the results of its solution utilizing this D – term modified approach.

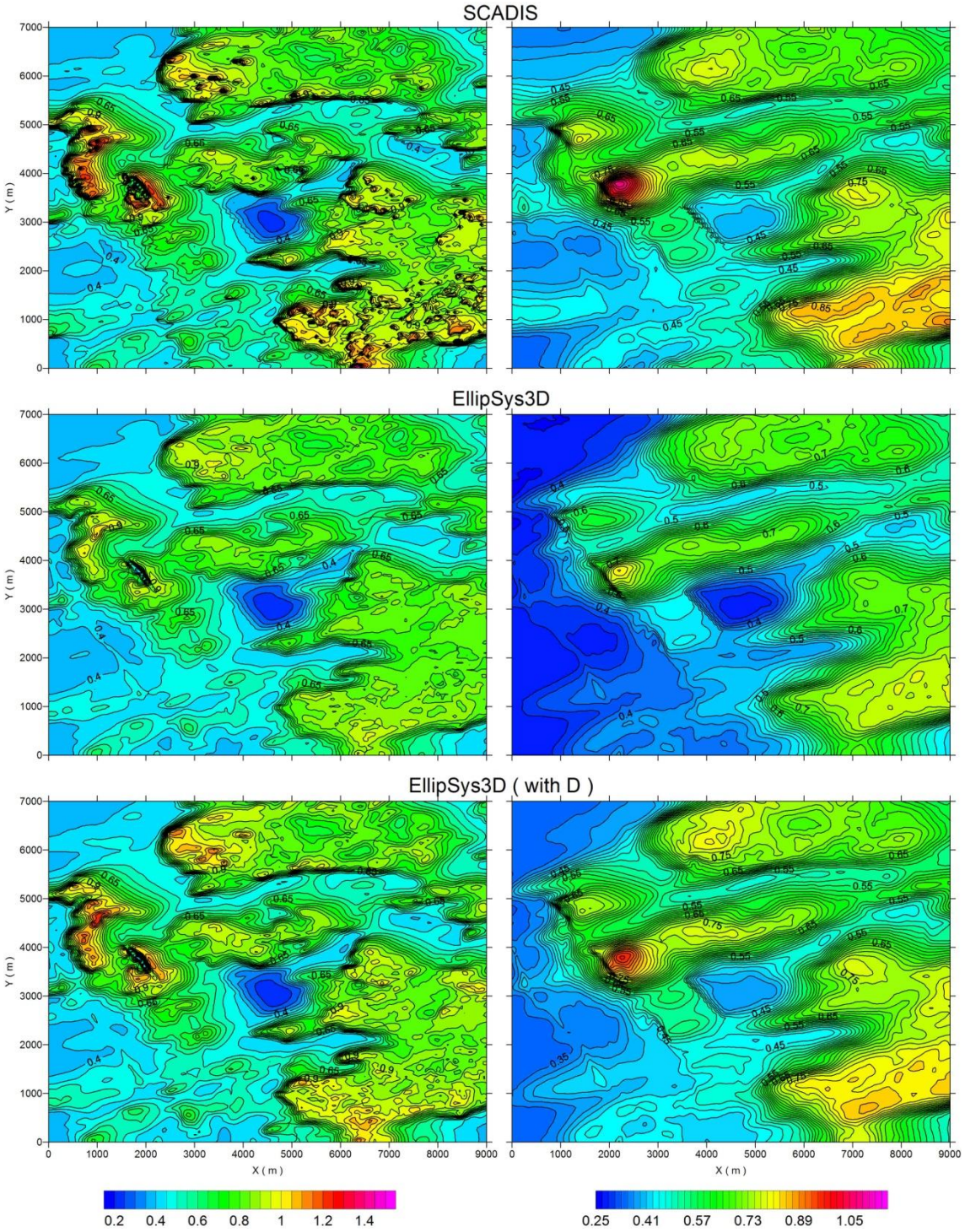

Fig.4. Simulated TKE ($m^2\ s^{-2}$) at 20 m AGL (on the left side) and at 50 m AGL (on the right side) over Østerild area using different models.

Performance of EllipSys3D with the canopy closure was also tested against observations. Before Østerild test station was erected, a number of measurements were made at different locations [18]. Results in Fig. 6 demonstrate the model ability to qualitatively reproduce the turbulence intensity measured during the campaign. Some deviation can be explained in part by uncertainties in canopy properties used in the model and in part by modelling issue itself, i.e.

TKE level and as such, turbulence intensity in the model depended on C_μ value, which is usually fixed, when in reality the value is a function of underlying surface properties. At present, the forest surrounding Østerild test station is partly cut [19]. However, the full information about forest properties is still unavailable. When such information becomes available, a unique opportunity to test model against airflow in changed conditions will exist.

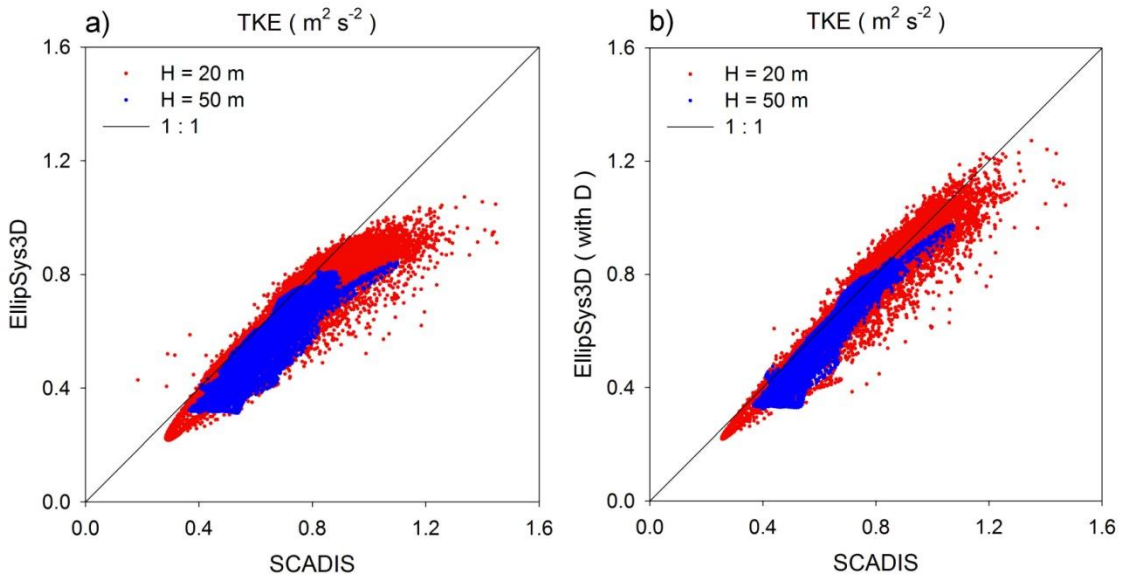

Fig. 5. TKE at 20 m AGL (red) and at 50 m AGL (blue) derived using the SCADIS model against that derived using the EllipSys3D model over computational domain. The 1 : 1 line is also shown.

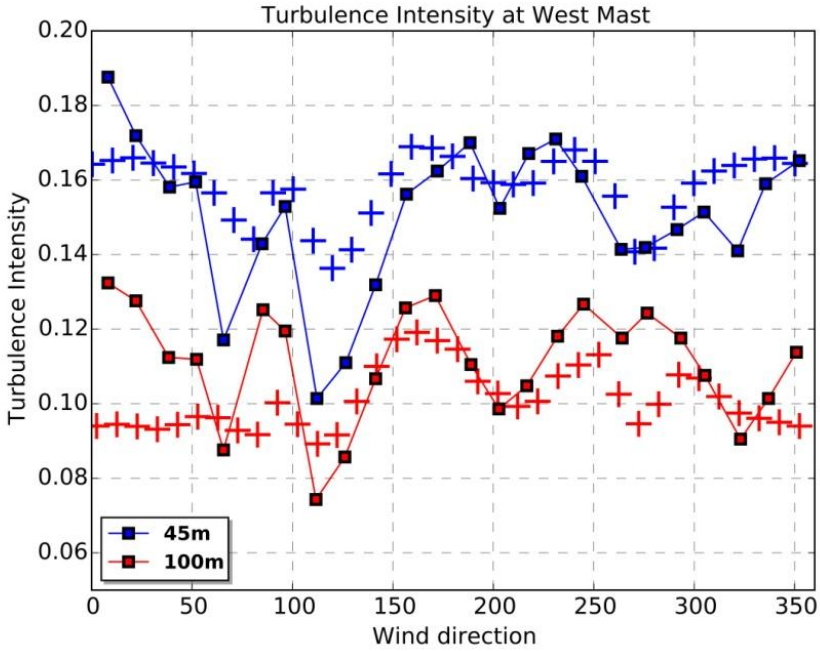

Fig. 6. Turbulent intensity measured (lines) and estimated using EllipSys3D (crosses) at the West station as a function of wind direction. Blue is for 45 m AGL and red is for 100 m AGL.

Conclusions

The present work assess the plant drag closure by comparing results of two in-house DTU Wind Energy models SCADIS and EllipSys3D against observations from the forested area of Østerild in Denmark. The numerical experiments show that the treatment of plant drag in the closure has universality and can be applied to any two-equation closure. Results derived by different CFD models with $k-\varepsilon$ and $k-\omega$ closures are similar and in good agreement with observations. Overall, numerical results show that the closure performs well, opening new possibilities for its application on tasks related to the atmospheric boundary layer – e.g. in cases where it is important to adequately account for influence of the vegetation.

References

[1]. Ayotte KW, Finnigan JJ, Raupach MR. “A second-order closure for neutrally stratified vegetative canopy flows”. *Boundary-Layer Meteorol* 1999;189-216.

[2]. Sogachev A, Panferov O. “Modification of two-equation models to account for plant drag”. *Boundary-Layer Meteorol* 2006; 121:229–266.

[3]. Pinard J-P, Wilson JD. “First- and second-order closure models for wind in a plant canopy”. *J Appl Meteorol* 2001; 40:1762–1768.

[4]. Hanjalić K. “Will RANS survive LES? A view of perspectives”. *ASME J Fluid Eng* 2005; 27:831–839.

[5]. Hanjalić K, Kenjereš S. “Some developments in turbulence modeling for wind and environmental engineering”. *J Wind Eng Ind Aerodyn* 2008; 96:1537-1570.

[6]. Apsley DD, Castro IP. “A limited-length-scale k - ε model for the neutral and stably-stratified atmospheric boundary layer”. *Boundary-Layer Meteorol* 1997; 83:75-98.

[7]. Sanz C. “A note on k–ε modelling of vegetation canopy air-flows”. *Boundary-Layer Meteorol* 2003; 108:191–197.

[8]. Sogachev A, Menzhulin G, Heimann M, Lloyd J. “A simple three dimensional canopy – planetary boundary layer simulation model for scalar concentrations and fluxes”. *Tellus* 2002; 54B:784-819.

[9]. Sogachev A, Kelly MC, Leclerc MY. “Consistent Two-Equation Closure Modelling for Atmospheric Research: Buoyancy and Vegetation Implementations”. *Boundary-Layer Meteorol* 2012;145(2):307-327.

[10]. Michelsen JA.”Basis3d – a platform for development of multiblock pde solvers”. *Technical report AFM 92-05*. Technical University of Denmark, 1992.

[11]. Sørensen NN. *Tech. Rep. Risø-R-827(EN)*, Risø National Laboratory, 2003; 154 pp.

[12]. Pope SB. *Turbulent flows*. Cambridge University Press, United Kingdom, 2000; 771 pp.

[13]. Raupach MR, Shaw RH. “Averaging procedures for flow within vegetation canopies”. *Boundary-Layer Meteorol* 1982; 22:79-90.

[14]. Finnigan JJ. “Turbulence in plant canopies”. *Annu Rev Fluid Mech* 2000; 32:519-571.

[15]. Sogachev A. “A note on two-equation closure modeling of canopy flow”. *Boundary-Layer Meteorol* 2009; 130:423–435.

[16]. Blackadar AK. “The vertical distribution of wind and turbulent exchange in a neutral atmosphere”. *J Geophys Res* 1962; 67:3095-3102.

[17]. Koblitz T, Bechmann A, Sogachev A, Sørensen NN, Réthoré P-E. "Computational Fluid Dynamics model of stratified atmospheric boundary-layer flow". *Wind Energy* 2015; 18(1): 75-89.

[18]. Mann J, Courtney M, Hummelshøj P, Jensen PH. ”Undersøgelse af vindforhold ved det kommende testcenter ved Østerild”. *Risø-R-1743 (DA)*, 2010; 31pp.

[19]. Brian O. Hansen BO,,Courtney M, Mortensen NG. ”Wind Resource Assessment – Østerild National Test Centre for Large Wind Turbines”. *DTU Wind Energy E-0052*, 2014, 46 pp.